NASA Technical Memorandum 100930

NASA-TM-100930 19880016051

Correlations of Velocity and Temperature Fluctuations in the Stagnation-Point Flow of Circular Cylinder in Turbulent Flow

Chi R. Wang
Lewis Research Center
Cleveland, Ohio

Prepared for the
1988 Winter Annual Meeting
of the American Society of Mechanical Engineers
Chicago, Illinois, November 28—December 2, 1988

NASA

CORRELATIONS OF VELOCITY AND TEMPERATURE FLUCTUATIONS IN THE STAGNATION-POINT FLOW OF CIRCULAR CYLINDER IN TURBULENT FLOW

Chi R. Wang
National Aeronautics and Space Administration
Lewis Research Center
Cleveland, Ohio 44135

ABSTRACT

Boundary layer flow and turbulence transport analyses to study the influence of the free-stream turbulence on the surface heat transfer rate and the skin friction around the stagnation point of a circular cylinder in a turbulent flow are presented. The analyses are formulated with the turbulent boundary layer equations, the Reynolds stress transport equations and the $k - \varepsilon$ two-equation turbulence modeling. The analyses are used to calculate the time-averaged turbulence double correlations, the mean flow properties, the surface heat transfer rate and the skin friction with an isotropic turbulence in the freestream. The analytical results are described and compared with the existing experimental measurements. Depending on the free-stream turbulence properties, the turbulence kinetic energy can increase or decrease as the flow moves toward the surface. However, the turbulence kinetic energy induces large Reynolds normal stresses at the boundary layer edge. The Reynolds normal stresses change the boundary layer profiles of the time-averaged double correlations of the velocity and temperature fluctuations, the surface heat transfer rate and the skin friction. The free-stream turbulence dissipation rate can affect the stagnation-point heat transfer rate but the influence of the free-stream temperature fluctuation on the heat transfer rate is insignificant.

INTRODUCTION

The predictions of the stagnation-point flow properties due to a circular cylinder in a turbulent flow are of practical importance in engineering applications. In the initial stage of the gas turbine blade design, the blade leading edge flow field is usually simulated with the results of the stagnation-point flow studies. Estimation of the blade leading edge surface heat transfer is an example. Much of the existing literature is focused on the study of the stagnation-point heat transfer rates. However, the influence of the free-stream turbulence on the mean velocity, the mean temperature and the turbulence double correlations near the stagnation point is critical to the prediction of the boundary layer flow development along the blade surface. Very limited results of the turbulence correlations and the mean flow properties within the stagnation-point flow were reported. This paper presents turbulence transport analyses of the velocity and the temperature fluctuations, the surface heat transfer rate and the skin friction within the stagnation-point flow of a circular cylinder in a turbulent freestream. The objective of this study is to establish analytically the stagnation-point boundary layer profiles of the mean velocity, the mean temperature and the time-averaged turbulence double correlations of the velocity and temperature fluctuations as functions of the turbulence intensity, the turbulence length scale (turbulence dissipation rate) and the Reynolds number of the freestream.

As in any turbulent flow analysis, modeling of the turbulence variation in the stagnation-point flow is a difficult task. The eddy viscosity concept was used in a turbulent boundary layer theory (Smith and Kuethe, 1966) to analyze the surface heat transfer rate and the skin friction of the stagnation-point flow field. In order to include the effect of the free-stream turbulence, the eddy viscosity was assumed to be proportional to the free-stream turbulence intensity. Following the progress of the turbulence modeling technique, Traci and Wilcox (1975) and Strahle (1985) analyzed the boundary layer edge turbulence conditions. They used the two-equation turbulence models to describe the turbulence kinetic energy variation along the stagnation-point streamline. Hijikata et al. (1982) added an equation for the anisotropic turbulence to the $k - \varepsilon$ turbulence modeling and numerically solved the Navier-Stokes equations for the Reynolds stress distributions along the stagnation-point streamline. It is generally agreed that a turbulence transport analysis using the Reynolds stress transport equations is a better approach to study the interaction between the turbulence and the mean flow strain. In a previous study (Wang and Yeh, 1987), Donaldson's turbulence modeling (Donaldson et al., 1972) and the $k - \varepsilon$ two-equation turbulence modeling (Launder and Spalding,

1974) were implemented with the boundary layer flow equations to analyze the influence of the free-stream turbulence on the surface heat transfer rate, the stagnation-point boundary layer profiles of the mean velocity, the mean temperature, and the time-averaged turbulence double correlations. The theoretical analyses of the previous study are used in this paper. However, the existing analyses are improved to model the variation of the time-averaged turbulence double correlations along the stagnation-point streamline and the boundary layer edge. The length scale for the turbulence closure assumptions are related analytically to the free-stream turbulence properties. The improved analyses are also used to investigate the influence of the free-stream temperature fluctuation on the stagnation-point heat transfer rate.

With the assumption of an isotropic turbulence in the freestream, the analyses are used to calculate numerically the time-averaged turbulence double correlations and the mean flow properties within the boundary layer around the stagnation point. The surface heat transfer rate and the skin friction are also calculated. These computational results are compared with the measurements of existing experiments to validate the present analyses.

NOMENCLATURE

a	mean velocity parameter
c_f	skin friction factor
c_i	empirical constants, $i = 1$ to 4
c_μ	empirical constant
D	cylinder diameter
E	dimensionless turbulence dissipation rate
F	dimensionless mean flow velocity component
G	transformed velocity of V
g	turbulence longitudinal correlation
H	dimensionless mean temperature
K_i	dimensionless turbulence kinetic energy, $i = 1$ to 3
k	turbulence kinetic energy
ℓ	spatial distance
Nu	Nusselt number
Pr	laminar Prandtl number, 0.7
R	sum of dimensionless Reynolds normal stresses
Re	Reynolds number
R_x	dimensionless Reynolds normal stress along x direction
R_y	dimensionless Reynolds normal stress along y direction
R_z	dimensionless Reynolds normal stress along z direction
S,τ	dimensionless Reynolds shear stress
T	mean temperature
Tu	free-stream turbulence intensity
t	temperature fluctuation
U,V	mean velocity components
u,v,w	velocity fluctuations
x,y,z	physical coordinate system
Δ	dimensionless length scale
ε	turbulence dissipation rate
η	transformed coordinate along y direction
Θ,θ	dimensionless turbulence correlation
Λ	turbulence modeling length scale
λ	turbulence longitudinal microlength scale
μ,ν	absolute and kinematic viscosity
ξ	transformed coordinate along x direction
ρ	density
φ	azimuth angle

Subscripts

e	boundary layer edge condition
F	free-stream condition
oe	boundary layer edge condition at initial station
W	surface condition
o	condition at initial station
1	condition at location 1
2	condition at location 2 of boundary layer edge

Superscript

$-$	time-averaged quantity

THEORETICAL FORMULATION

The theoretical model of the flow field is shown schematically in Fig. 1. The stagnation point 0 is taken as the coordinate-system origin with x and y coordinates parallel to and normal to the cylinder surface, respectively and z coordinate along the cylinder axis. The diameter of the cylinder is D and its axis is perpendicular to the free-stream mean velocity V_F. The mean flow is assumed to be steady, incompressible, and two-dimensional. The mean velocity components are U and V along the x and y directions. The turbulent velocity fluctuations along the x, y, and z directions are denoted by u, v, and w. The free-stream Reynolds number is defined as $Re = V_F D/\nu$, where ν is the kinematic viscosity. The free-stream turbulence is characterized by its turbulence intensity $Tu = \left(\overline{v_F^2}\right)^{1/2} / V_F$ and its turbulence dissipation rate

ϵ_F. The free-stream mean temperature is T_F. The cylinder surface is at a constant temperature T_W.

The following hypotheses are used in developing the theoretical formulation. A boundary layer flow is assumed to exist along the surface around the stagnation point. The mean velocity in the external flow is represented by the result of the inviscid flow analysis around a circular cylinder. The turbulence is distorted as the flow moves toward the stagnation point and the turbulence conditions, different from those in the freestream, are imposed along the boundary layer edge. The turbulence boundary layer edge conditions induce turbulence momentum and thermal fluxes within the boundary layer. These turbulence fluxes influence the boundary layer mean flow properties, the surface heat transfer rate and the skin friction. Based on the above hypotheses, the following theoretical models are proposed to investigate the momentum and thermal interaction within the stagnation-point flow field.

Boundary Layer Flow Analysis

Similar to the analyses in the previous study (Wang and Yeh, 1987), the mean flow properties within the boundary layer are described by the two-dimensional boundary layer equations. The turbulence flux terms in momentum and enthalpy equations are modeled with the time-averaged turbulence transport equations. The mean flow properties and the turbulence double correlations are nondimensionalized and they are defined as

$$F = \frac{U}{U_e}, \quad H = \frac{T}{T_e}$$

$$R_x = \frac{\overline{u^2}}{U_e^2}, \quad R_y = \frac{\overline{v^2}}{U_e^2}, \quad R_z = \frac{\overline{w^2}}{U_e^2}$$

$$S = \frac{-\overline{uv}}{U_e^2}, \quad \Theta = \frac{-\overline{vt}}{U_e T_e}.$$

The physical coordinates x and y are also transformed into the dimensionless coordinate system ξ and η by using the following relations:

$$\xi = \int_0^x \frac{U_e}{\nu}\, dx \quad \text{and} \quad \eta = \frac{\frac{U_e y}{\nu}}{(2\xi)^{0.5}} \tag{1}$$

It is further assumed that the turbulence does not influence the mean velocity within the external flow region and its mean velocity is represented with the two-dimensional inviscid flow solution due to a circular cylinder in a uniform freestream. The mean velocity components are

$$U = ax \quad \text{and} \quad V = -ay \tag{2}$$

with $a = 4V_F/D$.

Therefore, the governing equations for the mean flow and the turbulence become

Continuity equation,

$$2\xi \frac{\partial F}{\partial \xi} + \frac{\partial G}{\partial \eta} + F = 0 \tag{3}$$

where $G = \frac{2\xi\nu F}{U_e}\frac{\partial \eta}{\partial X} + (2\xi)^{0.5}\frac{V}{U_e}$

Momentum equation,

$$2\xi F \frac{\partial F}{\partial \xi} + G\frac{\partial F}{\partial \eta} = \frac{2\xi(1 - F^2)}{U_e}\frac{\partial U_e}{\partial \xi} + \frac{\partial^2 F}{\partial \eta^2} + (2\xi)^{0.5}\frac{\partial S}{\partial \eta} \tag{4}$$

Enthalpy equation,

$$2\xi F \frac{\partial H}{\partial \xi} + G\frac{\partial H}{\partial \eta} = -\frac{2\xi F H}{T_e}\frac{\partial T_e}{\partial \xi} + \frac{1}{Pr}\frac{\partial^2 H}{\partial \eta^2} + (2\xi)^{0.5}\frac{\partial \Theta}{\partial \eta} \tag{5}$$

Turbulence transport equations,

$$2\xi F \frac{\partial R_x}{\partial \xi} + G\frac{\partial R_x}{\partial \eta} = -2\xi \frac{4R_x F}{U_e}\frac{\partial U_e}{\partial \xi} + \frac{U_e}{\nu}\frac{\partial}{\partial \eta}\left(\Lambda R^{0.5}\frac{\partial R_x}{\partial \eta}\right)$$
$$+ \frac{\partial^2 R_x}{\partial \eta^2} + 2S(2\xi)^{0.5}\frac{\partial F}{\partial \eta} + 2\xi\frac{(R - 3R_x)}{3}\frac{\nu R^{0.5}}{\Lambda U_e}$$
$$+ 2\xi R_x\left(-2\frac{\partial F}{\partial \xi} - \frac{2\nu}{U_e}\frac{\partial F}{\partial \eta}\frac{\partial \eta}{\partial X} - \frac{2\nu^2}{U_e^2\Lambda^2}\right) \tag{6}$$

$$2\xi F \frac{\partial R_y}{\partial \xi} + G\frac{\partial R_y}{\partial \eta} = 5\frac{U_e}{\nu}\frac{\partial}{\partial \eta}\left(\Lambda R^{0.5}\frac{\partial R_y}{\partial \eta}\right) + \frac{\partial^2 R_y}{\partial \eta^2}$$
$$+ 2\xi\frac{\nu R^{0.5}}{\Lambda U_e}\frac{(R - 3R_y)}{3}$$
$$+ 2\xi R_y\left(2\frac{\partial F}{\partial \xi} + \frac{2\nu}{U_e}\frac{\partial F}{\partial \eta}\frac{\partial \eta}{\partial x} - \frac{2\nu^2}{\Lambda^2 U_e^2}\right) \tag{7}$$

$$2\xi F \frac{\partial R_z}{\partial \xi} + G\frac{\partial R_z}{\partial \eta} = -2\xi \frac{2R_z F}{U_e}\frac{\partial U_e}{\partial \xi} + \frac{U_e}{\nu}\frac{\partial}{\partial \eta}\left(\Lambda R^{0.5}\frac{\partial R_z}{\partial \eta}\right)$$
$$+ \frac{\partial^2 R_z}{\partial \eta^2} + 2\xi\frac{\nu R^{0.5}}{\Lambda U_e}\frac{(R - 3R_z)}{3} - 2\xi R_z\frac{2\nu^2}{\Lambda^2 U_e^2} \tag{8}$$

$$2\xi F \frac{\partial S}{\partial \xi} + G\frac{\partial S}{\partial \eta} = -2\xi\frac{2SF}{U_e}\frac{\partial U_e}{\partial \xi} + 3\frac{U_e}{\nu}\frac{\partial}{\partial \eta}\left(\Lambda R^{0.5}\frac{\partial S}{\partial \eta}\right) + \frac{\partial^2 S}{\partial \eta^2}$$
$$+ (2\xi)^{0.5} R_y\frac{\partial F}{\partial \eta} + 2\xi S\left(-\frac{\nu R^{0.5}}{\Lambda U_e} - \frac{2\nu^2}{\Lambda^2 U_e^2}\right) \tag{9}$$

and

$$2\xi F \frac{\partial \Theta}{\partial \xi} + G\frac{\partial \Theta}{\partial \eta} = -2\xi\frac{\Theta F}{T_e}\frac{\partial T_e}{\partial \xi} + 3\frac{U_e}{\nu}\frac{\partial}{\partial \eta}\left(\Lambda R^{0.5}\frac{\partial \Theta}{\partial \eta}\right)$$
$$+ \frac{\partial^2 \Theta}{\partial \eta^2} + (2\xi)^{0.5} R_y\frac{\partial H}{\partial \eta}$$
$$+ 2\xi\Theta\left(\frac{\partial F}{\partial \xi} + \frac{\nu}{U_e}\frac{\partial F}{\partial \eta}\frac{\partial \eta}{\partial x} - \frac{\nu R^{0.5}}{\Lambda R_e} - \frac{2\nu^2}{\Lambda^2 U_e^2}\right) \tag{10}$$

where $R = R_x + R_y + R_z$.

The above governing equations were derived in the previous work (Wang and Yeh, 1987) by following the theoretical analyses by Donaldson et al. (1972) and Beckwith and Bushnell (1966). A length scale Λ was used in the closure assumptions for the time-averaged higher-order turbulence correlations. In this study, the following linear relations are assumed for the length scale within the boundary layer,

$$\left.\begin{aligned} \Lambda &= y, \quad \text{for} \quad 0 \le y \le y_p \\ \Lambda &= \Lambda_p + (y - y_p)\left(\frac{\Lambda_e - \Lambda_p}{y_e - y_p}\right) \quad \text{for} \quad y_p \le y \le y_e \end{aligned}\right\} \tag{11}$$

where y_p is a very small distance ($= 0.02\, y_e$) from the surface. The subscript p denotes the pivot-point locations.

Along the stagnation-point streamline, the upstream limit η_1 of the external flow region is defined by matching the mean flow velocity, i.e., $V_1 = V_F$ at $\eta = \eta_1$. The downstream limit η_2 is defined by matching the turbulence conditions at the boundary layer edge.

The boundary layer edge conditions of the turbulence double correlations are analyzed with the turbulence transport equations. For this purpose, the following conditions

$$F = 1, \quad H = 1, \quad \frac{\partial R_x}{\partial \eta} = 0, \quad \frac{\partial R_y}{\partial \eta} = 0, \quad \frac{\partial R_z}{\partial \eta} = 0,$$

$$\frac{\partial S}{\partial \eta} = 0, \quad \text{and} \quad \frac{\partial \Theta}{\partial \eta} = 0, \tag{12}$$

are assumed at the locations near the boundary layer edge.

Nonslip conditions

$$F = 0, \quad H = \frac{T_w}{T_e}, \quad R_x = 0, \; R_y = 0, \quad R_z = 0,$$

$$S = 0, \quad \text{and} \quad \Theta = 0 \tag{13}$$

are imposed along the cylinder surface $\eta = 0$. Based on the above boundary conditions, Eqs. (3) to (10) are used in this study to model the mean flow properties and the turbulence double correlations.

Stagnation-Point Streamline Turbulence

The turbulence double correlations along the stagnation-point streamline within the external flow region are modeled with Donaldson's turbulence modeling technique. With the mean flow velocity assumption, Eq. (2), the turbulence transport equation becomes

$$\frac{d^2K_1}{d\eta^2} + \frac{d}{d\eta}\left(\Delta K^{0.5}\frac{dK_1}{d\eta}\right) + \eta\frac{dK_1}{d\eta} - K_1\left(2 + \frac{K^{0.5}}{\Delta} + \frac{2}{\Delta^2}\right) + \frac{K^{1.5}}{3\Delta} = 0 \tag{14}$$

$$\frac{d^2K_2}{d\eta^2} + 5\frac{d}{d\eta}\left(\Delta K^{0.5}\frac{dK_2}{d\eta}\right) + \eta\frac{dK_2}{d\eta} - K_2\left(-2 + \frac{K^{0.5}}{\Delta} + \frac{2}{\Delta^2}\right) + \frac{K^{1.5}}{3\Delta} = 0 \tag{15}$$

$$\frac{d^2K_3}{d\eta^2} + \frac{d}{d\eta}\left(\Delta K^{0.5}\frac{dK_3}{d\eta}\right) + \eta\frac{dK_3}{d\eta} - K_3\left(\frac{K^{0.5}}{\Delta} + \frac{2}{\Delta^2}\right) + \frac{K^{1.5}}{3\Delta} = 0 \tag{16}$$

$$\frac{d^2\tau}{d\eta^2} + 3\frac{d}{d\eta}\left(\Delta K^{0.5}\frac{d\tau}{d\eta}\right) + \eta\frac{d\tau}{d\eta} - \tau\left(\frac{K^{0.5}}{\Delta} + \frac{2}{\Delta^2}\right) = 0 \tag{17}$$

and

$$\frac{d^2\Theta}{d\eta^2} + 3\frac{d}{d\eta}\left(\Delta K^{0.5}\frac{d\Theta}{d\eta}\right) + \eta\frac{d\Theta}{d\eta} - \Theta\left(-1 + \frac{K^{0.5}}{\Delta} + \frac{2}{\Delta^2}\right) = 0 \tag{18}$$

Where K_1, K_2, K_3, τ, Θ, and Δ are the dimensionless turbulence double correlations and length scale. They are defined as

$$K_1 = \frac{\overline{u^2}}{a\nu}, \quad K_2 = \frac{\overline{v^2}}{a\nu}, \quad K_3 = \frac{\overline{w^2}}{a\nu}, \quad \tau = \frac{-\overline{uv}}{a\nu},$$

$$\Theta = \frac{-\overline{vt}}{k_F^{0.5}T_F}, \quad \text{and} \quad \Delta = \frac{\Lambda}{\left(\frac{\nu}{a}\right)^{0.5}}$$

with $K = K_1 + K_2 + K_3$.

The free-stream turbulence properties are the turbulence conditions at η_1. Therefore, at η_1,

$$K_1 = K_{1,F}, \quad K_2 = K_{2,F}, \quad K_3 = K_{3,F}, \quad \tau = 0,$$

$$\Theta = \Theta_F \tag{19}$$

The turbulence conditions at η_2 were described in Eq. (11). However, the Reynolds normal stress gradients at η_2 are replaced by their corresponding Reynolds normal stresses. The following analysis is used to determine these normal stress components.

Applying the assumptions in Eq. (12) to the turbulence transport Eqs. (6) to (10) results in the following expressions for the gradients of the turbulence correlations along the ξ direction

$$\frac{\partial R_{x,e}}{\partial \xi} = R_{x,e}\left(-\frac{4}{U_e}\frac{dU_e}{d\xi} - \frac{\nu R_e^{0.5}}{\Lambda_e U_e} - \frac{2\nu^2}{U_e^2\Lambda_e^2}\right) + \frac{1}{3}\frac{\nu R_e^{1.5}}{\Lambda_e U_e} \tag{20}$$

$$\frac{\partial R_{y,e}}{\partial \xi} = R_{y,e}\left(-\frac{\nu R_e^{0.5}}{\Lambda_e U_e} - \frac{2\nu^2}{U_e^2\Lambda_e^2}\right) + \frac{1}{3}\frac{\nu R_e^{1.5}}{\Lambda_e U_e} \tag{21}$$

$$\frac{\partial R_{z,e}}{\partial \xi} = R_{z,e}\left(-\frac{2}{U_e}\frac{dU_e}{d\xi} - \frac{\nu R_e^{0.5}}{\Lambda_e U_e} - \frac{2\nu^2}{U_e^2\Lambda_e^2}\right) + \frac{1}{3}\frac{\nu R_e^{1.5}}{\Lambda_e U_e} \tag{22}$$

$$\frac{\partial S}{\partial \xi} = S_e\left(-\frac{2}{U_e}\frac{dU_e}{d\xi} - \frac{\nu R_e^{0.5}}{\Lambda_e U_e} - \frac{2\nu^2}{U_e^2\Lambda_e^2}\right) \tag{23}$$

and

$$\frac{\partial \Theta}{\partial \xi} = \Theta_e\left(-\frac{1}{T_e}\frac{dT_e}{d\xi} - \frac{\nu R_e^{0.5}}{\Lambda_e U_e} - \frac{2\nu^2}{U_e^2\Lambda_e^2}\right) \tag{24}$$

It is assumed that, within the boundary layer thickness in the vicinity of the stagnation point, the Reynolds normal stresses are independent of φ. Therefore,

$$\frac{\partial R_{x,e}}{\partial \xi} = \frac{-2R_{x,e}}{Re\varphi^2}, \quad \frac{\partial R_{y,e}}{\partial \xi} = \frac{-2R_{y,e}}{Re\varphi^2}, \quad \text{and}$$

$$\frac{\partial R_{z,e}}{\partial \xi} = \frac{-2R_{z,e}}{Re\varphi^2} \tag{25}$$

are found at $\varphi \doteq 0$.

Substituting the above relations into Eqs. (20) to (22) and rearranging the equations leads to the following expressions

$$R_{x,oe} = \frac{\frac{1}{3}\frac{\nu R_{oe}^{1.5}}{\Lambda_{oe}U_{oe}}}{\frac{-2}{Re\varphi_o^2} + \frac{4(dU_e/d\xi)_{oe}}{U_{oe}} + \frac{\nu R_{oe}^{0.5}}{\Lambda_{oe}U_{oe}} + \frac{2\nu^2}{U_{oe}^2\Lambda_{oe}^2}} \tag{26}$$

$$R_{y,oe} = \frac{\frac{1}{3}\frac{\nu R_{oe}^{1.5}}{\Lambda_{oe}U_{oe}}}{\frac{-2}{Re\varphi_o^2} + \frac{\nu R_{oe}^{0.5}}{\Lambda_{oe}U_{oe}} + \frac{2\nu^2}{U_{oe}^2\Lambda_{oe}^2}} \tag{27}$$

and

$$R_{z,oe} = \frac{\frac{1}{3}\frac{\nu R_{oe}^{1.5}}{\Lambda_{oe}U_{oe}}}{\frac{-2}{Re\varphi_o^2} + \frac{2(dU_e/d\xi)_{oe}}{U_{oe}} + \frac{\nu R_{oe}^{0.5}}{\Lambda_{oe}U_{oe}} + \frac{2\nu^2}{U_{oe}^2\Lambda_{oe}^2}} \tag{28}$$

for the Reynolds normal stresses at $\varphi_o \approx 0$ and $\eta = \eta_2$. To be consistant with the definitions of the variables in Eqs. (14) to (18), the above relations are rewritten as

$$K_{1,oe} = \frac{\frac{1}{3}\frac{\nu a K_{oe}^{1.5}}{\Delta_{oe}U_{oe}^2}}{\frac{-2}{Re\varphi_o^2} + \frac{\nu a K_{oe}^{0.5}}{\Delta_{oe}U_{oe}^2} + \frac{2\nu a}{U_{oe}^2\Delta_{oe}^2} + \frac{4(dU_e/d\xi)_{oe}}{U_{oe}}} \tag{29}$$

$$K_{2,oe} = \frac{\frac{1}{3}\frac{\nu a K_{oe}^{1.5}}{\Delta_{oe}U_{oe}^2}}{\frac{-2}{Re\varphi_o^2} + \frac{\nu a K_{oe}^{0.5}}{\Delta_{oe}U_{oe}^2} + \frac{2\nu a}{U_{oe}^2\Delta_{oe}^2}} \tag{30}$$

and

$$K_{3,oe} = \frac{\frac{1}{3}\frac{\nu a K_{oe}^{1.5}}{\Delta_{oe}U_{oe}^2}}{\frac{-2}{Re\varphi_o^2} + \frac{\nu a K_{oe}^{0.5}}{\Delta_{oe}U_{oe}^2} + \frac{2\nu a}{U_{oe}^2\Delta_{oe}^2} + \frac{2(dU_e/d\xi)_{oe}}{U_{oe}}} \tag{31}$$

Equations (29) to (31), $d\tau/d\eta = 0$, and $d\theta/d\eta = 0$ are the final forms of the turbulence boundary conditions at η_2. With the turbulence boundary conditions at η_1 and η_2, Eqs. (14) to (18) are used to model the turbulence double correlations at locations between η_1 and η_2. A constant Δ_{oe} is also assumed in this region. This length scale is determined by the requirement that

$$K_{oe} = K_{1,oe} + K_{2,oe} + K_{3,oe} \tag{32}$$

The $k - \varepsilon$ two-equation turbulence modeling is used to define K_{oe}. Based on the previous analysis (Wang and Yeh, 1987), the k and ε equations are written as

$$\eta\frac{dK}{d\eta} = -2c_\mu\frac{K^2}{E} + 2E - \frac{d}{d\eta}\left(c_\mu\frac{K}{4c_3E}\frac{dK}{d\eta}\right) \tag{33}$$

$$\eta\frac{dE}{d\eta} = -2c_1c_\mu K + 2c_2\frac{E^2}{K^2} - \frac{d}{d\eta}\left(c_\mu\frac{K}{4c_4E}\frac{dE}{d\eta}\right) \tag{34}$$

with

$$K = \frac{2k}{\nu a} \quad \text{and} \quad E = \frac{\varepsilon}{\nu a^2}.$$

The boundary conditions are

$$K = \frac{2k_F}{\nu a}, \quad E = \frac{\varepsilon_F}{\nu a^2}, \quad \frac{dE}{d\eta} = \frac{2}{\eta}\left(c_2\frac{E^2}{K} - c_1c_\mu K\right) \quad \text{at} \quad \eta_1.$$

and

$$\frac{dK}{d\eta} = 0 \quad \text{at} \quad \eta_2.$$

The empirical constants are $c_1 = 1.44$, $c_2 = 1.92$, $c_3 = 1.00$, $c_4 = 1.30$, and $c_\mu = 0.09$.

The above boundary value problem defines the turbulence kinetic energy K in $\eta_1 \geq \eta \geq \eta_2$ along the stagnation-point streamline. The previous work (Wang and Yeh, 1987) also indicated that the boundary layer edge was located at $\eta_2 \approx 5$. Once the turbulence kinetic energy K_{oe} is obtained, $K_{1,oe}$, $K_{2,oe}$,

$K_{3,oe}$, and Λ_{oe} can be found by solving Eqs. (29) to (32).

The previous analysis (Wang and Yeh, 1987) is also used to model the initial profiles of the turbulence in $\eta_2 \geq \eta > 0$. The turbulence correlation gradient terms in ξ-direction are also assumed to be independent of η and they are represented by Eqs. (20) to (24). Due to symmetry in the mean flow, $\partial F/\partial\xi = 0$ and $\partial H/\partial\xi = 0$ are true along the stagnation-point streamline. Substituting these mean flow streamwise gradients into Eqs. (3) to (10) results in a set of ordinary differential equations which describe the variations of the mean flow properties and the turbulence double correlations in $\eta_2 \geq \eta \geq 0$. Equations (12) and (13) express the boundary conditions at $\eta = 0$ and η_2.

Boundary Layer Edge Turbulence

Equations (3) to (10) are also used to model the turbulence double correlations within the boundary layer flow around the stagnation point. The initial profiles of the mean flow properties and the turbulence double correlations within the boundary layer thickness along the stagnation-point streamline were defined from the analysis in the previous sections. The surface boundary conditions were also described by Eq. (13). The boundary layer edge mean flow properties are $F = 1$ and $H = 1$. Thus, the boundary layer edge turbulence conditions are required to form a complete set of the mean flow and turbulence boundary conditions for Eqs. (3) to (10). Analysis of the boundary layer edge turbulence conditions is described in the following.

The $\kappa - \varepsilon$ two-equation turbulence modeling is used again to predict the turbulence kinetic energy along the boundary layer edge. Following the previous analysis (Wang and Yeh, 1987), the k and ε equations are written as

$$\xi \frac{dK}{d\xi} = c_\mu \frac{K^2}{E} - E + \xi \frac{d}{d\xi}\left(c_\mu \frac{K^2}{4c_3 E} \frac{dK}{d\xi}\right) \qquad (35)$$

$$\xi \frac{dE}{d\xi} = c_1 c_\mu K - c_2 \frac{E^2}{K} + \xi \frac{d}{d\xi}\left(c_\mu \frac{K^2}{2c_4 E} \frac{dE}{d\xi}\right) \qquad (36)$$

with

$$K = \frac{2k}{\nu a} \quad \text{and} \quad E = \frac{\varepsilon}{\nu a^2} .$$

The analysis along the stagnation-point streamline provides the K and E initial conditions at (ξ_2, η_2). Equations (35) and (36) are solved by numerical iteration for the boundary layer edge turbulence kinetic energy within the small region $\varphi \leq 10°$. Equations (20) to (24) are also integrated numerically to calculate the downstream boundary layer edge turbulence kinetic energy (or the corresponding Reynolds normal stresses). The length scale Λ_e is not necessarily constant along the boundary layer edge. Through numerical iteration, this local length scale Λ_e is found such that the sum of the Reynolds normal stresses converges to the local turbulence kinetic energy obtained from eqs. (35) and (36). The local Reynolds normal stresses are the boundary layer edge turbulence conditions.

NUMERICAL COMPUTATION

Most of the numerical computational procedures used in this study were described in the previous work (Wang and Yeh, 1987). These existing numerical computational procedures were performed to verify the present theoretical formulation. This verification is also based on existing experiments. Several sets of the experimental data on the effect of the free-stream turbulence on the heat transfer rate from a heated cylinder placed normal to airstream were reported by Smith and Kuethe (1966), Lowery and Vachon (1975), and Zukauskas and Ziugzda (1985). Honeycomb structure, damping screens or turbulence inducing grids at various locations upstream of the test cylinder provided variations in the free-stream turbulence conditions. The measurements of the two-point turbulence longitudinal double correlations in the free stream were also reported by Lowery and Vachon (1975). The two-point turbulence correlations provide information regarding the free-stream turbulence dissipation rate. Therefore, their test conditions and results are first used to validate the present theoretical formulation. Assuming the free-stream turbulence is isotropic, the free-stream turbulence kinetic energy and turbulence dissipation rate are described (Hinze, 1975) by

$$k_F = \frac{3\overline{v_F^2}}{2} \quad \text{and} \quad \varepsilon_F = \frac{30\nu\overline{v_F^2}}{\lambda_F^2} \qquad (37)$$

The longitudinal two-point turbulence correlation g, the spatial distance ℓ, and the turbulence longitudinal microlength scale λ_F are related by the following relations for small ℓ

$$g(\ell) = 1 - \frac{\ell^2}{\lambda_F^2} \qquad (38)$$

The turbulence longitudinal microlength scales are obtained by curve-fitting the experimental data with Eq. (38). Based on the free-stream mean velocity, the free-stream turbulence intensity, and the turbulence longitudinal microlength scale, the present analysis is used to calculate numerically the turbulence double correlations and the mean flow properties within the stagnation-point flow field. The surface heat transfer rate and the skin friction are then determined from the mean velocity and the mean temperature profiles.

Summary of the computational sequences associated with the present theoretical formulation are presented here. The computational sequences are:

(1) The $k - \varepsilon$ two-equation turbulence modeling, Eqs. (33) and (34), were solved for the turbulence kinetic energy K in $\eta_1 \geq \eta \geq \eta_2$. The turbulence kinetic energy at η_2 was substituted into Eqs. (29) to (31) to solve for the turbulence kinetic energy $K_{1,oe}$, $K_{2,oe}$, and $K_{3,oe}$ by numerical iteration in terms of the length scale Δ_{oe}. The length scale Δ_{oe} was chosen such that the resulting turbulence double correlations satisfied Eq. (32).

(2) Turbulence kinetic energy in $\eta_1 \geq \eta \geq \eta_2$ and the length scale Δ_{oe} were used to linearize the finite difference equations corresponding to Eqs. (14) to (16). The finite difference equations were obtained by using central finite difference approximation. Since the Reynolds normal stresses were specified at $\eta_1 \geq \eta \geq \eta_2$, these finite difference equations were solved with the method of successive substitution. These Reynolds normal stress distributions were used to calculate τ and

θ in $\eta_1 \geq \eta \geq \eta_2$ from the finite difference equations corresponding to Eqs. (17) and (18). The free-stream condition $\tau = 0$ and an arbitrary boundary condition $\theta = \theta_F$ were imposed at η_1 in order to study the effect of the correlation of the free-stream velocity and temperature fluctuations on the surface heat transfer rate. These finite difference equations were solved by using the method of the matrix inversion. Variable grid dimension was used in numerical computation. Two hundred grid points were used. The grid was tightened near η_1 and η_2 to ensure the boundary conditions.

(3) The turbulence double correlations at (ξ_2,η_2) were substituted into Eqs. (20) to (24) to determine the ξ-direction gradients. The mean flow conditions were calculated at $\varphi = 0.01°$ location. Introducing the ξ-direction gradients into Eqs. (3) to (10) led to a set of ordinary differential equations with the boundary conditions specified at $\eta = 0$ and η_2. These equations were then solved numerically for the mean flow properties and the turbulence correlations. It was also found that the choice of $\varphi (\approx 0°)$ other than 0.01° did not significantly change the results of the numerical computations. This computational step and step 2 calculated the turbulent flow properties along the stagnation-point streamline.

(4) Based on the Reynolds normal stresses at (ξ_2,η_2), Eqs. (35) and (36) were solved numerically for the turbulence kinetic energy along the boundary layer edge. A fourth-order Runge-Kutta numerical method was used to integrate Eqs. (20) to (24) for the downstream turbulence double correlations. Very small step size in ($\Delta\xi$ corresponding to $\Delta\varphi = 0.001°$) was used. The numerical integration at any location ξ was performed iteratively in terms of the length scale Λ_e. The iteration procedure was terminated when the sum of the Reynolds normal stresses converged to the turbulence kinetic energy previously obtained from Eqs. (35) and (36). Since $\tau = 0.$ and $\theta = 0.$ were calculated at (ξ_2,η_2), Eqs. (23) and (24) showed that $\tau = 0.$ and $\theta = 0.$ also occurred along the downstream boundary layer edge.

(5) Finally, the properties of the mean flow and the turbulence double correlations within the boundary layer flow around the stagnation point ($\varphi \lesssim 10°$) were calculated from Eqs. (3) to (10) by using an existing downstream marching numerical computational scheme. The Nusselt number Nu and the skin friction factor c_f were then calculated from the mean velocity and the mean temperature profiles. They are defined as

$$Nu = -D\left(\frac{\partial T}{\partial y}\right)_{y=0} \Big/ (T_W - T_F)$$

and

$$c_f = \mu\left(\frac{\partial U}{\partial y}\right)_{y=0} \Big/ \left(\frac{1}{2}\rho_F V_F^2\right)$$

The mean velocity and mean temperature gradients at the surface were calculated numerically from the mean velocity and mean temperature profiles which were previously obtained from the boundary layer flow solutions.

RESULTS AND DISCUSSIONS

The numerical computational procedures were performed for several cases with different free-stream turbulence conditions. Examples of the freestream turbulence longitudinal double correlations and the turbulence microlength scale are shown in Fig. 2. Some of the present computational results are described in the following sections and these results are also compared with available experimental measurements.

Turbulence

The variations of the dimensionless Reynolds normal stresses along the stagnation-point streamline are shown in Figs. 3(a) and (b). Rapid changes in the normal stresses occur near η_1. For most cases, the normal stress components K_1 and K_3 decrease and K_2 increases along the stagnation-point streamline within the external flow region. Within the boundary layer, the Reynolds normal stresses decrease continuously in the direction toward the surface. Large K_2 and small K_1 and K_3 were predicted at locations close to the surface. Figure 3(b) also shows that, with $Tu = 0.028$, $Re = 2.52\times10^5$, and $\lambda_F/D = 0.0079$, the normal stresses amplify along the stagnation-point streamline within the external flow and the maximum normal stresses occur at the boundary layer edge.

The profiles of the dimensionless shear stress $-\overline{uv}/v_a$ and the dimensionless mean velocity U/U_e within the boundary layer thickness along the stagnation-point streamline are shown in Figs. 4(a) and (b). With the prescribed free-stream turbulence longitudinal microlength scales, these results show that large shear stress was predicted within the boundary layer for the case with large Tu or Re. Increasing Tu or Re increases U/U_e within the region close to the surface and decreases U/U_e at locations near the boundary layer edge. The existing measurements (Kestin and Richardson, 1969) of U/U_e with $Tu = 0.05$ and $Re = 2.30\times10^5$ were also plotted in Fig. 4(a) to compare with the present analytical results of U/U_e. Following the test conditions of Lowery and Vachon (1975), $Re = 1.11\times10^5$ and $\lambda_F/D = 0.0086$ were used in the present numerical calculation and the present analysis predicted a smaller U/U_e in the region near the surface and a larger U/U_e at locations near the boundary layer edge.

The dimensionless turbulence correlation $-\overline{vt}/k_F^{0.5}T_F$ and mean temperature T/T_F along the stagnation-point streamline are shown in Figs. 5(a) and (b). The turbulence correlation $-\overline{vt}$ decays rapidly within the external flow and $-\overline{vt} = 0$ occurs at the boundary layer edge. This turbulence correlation appears again within the boundary layer. It increases to a maximum value near the surface and then decreases to the non-slip surface condition. With the prescribed turbulence longitudinal microlength scale, increasing the free-stream turbulence intensity changes the $-\overline{vt}$ and T profiles within the boundary layer and increases the mean temperature gradient at the surface. Therefore, the turbulent freestream induces a larger surface heat transfer rate than that with a laminar free-stream condition.

Analytical results of the Reynolds normal stresses and the length scales for the turbulence closure assumptions along the boundary layer edge are shown in Figs. 6(a) and (b). The Reynolds normal stresses remain constant near the stagnation point and then increase continuously at the downstream locations. The turbulence is anisotropic and the component $K_{2,e}$ is the largest among the Reynolds normal stresses. Constant length scale Δ_e was predicted for the cases with large Tu or large Re. The length scale increases slightly at the downstream locations for the case with a small Tu. In the analysis of the boundary layer edge turbulence, the turbulence kinetic energy was determined by solving Eqs. (33) and (34). The

diffusion terms are retained in these equations. Examinations of the present computational results indicate that the production and the diffusion terms in Eqs. (33) and (34) are the dominant terms in the turbulence development. The diffusion term is very small except at the locations very near the stagnation point. Therefore, the present computational results from Eqs. (33) and (34) are consistent with the boundary layer flow assumption.

The computational results of the Reynolds normal stresses within the boundary layer at $\varphi = 0°$, 5°, and 10° are shown in Figs. 7(a) and (b). These results indicate that large Reynolds normal stresses occur at the boundary layer edge and the normal stresses decrease continuously along the direction toward the surface. The components K_1 and K_3 increase as the flow moves downstream. Within a small region near the surface, the K_2 component decreases at the locations near the stagnation point and it increases again at the downstream locations. These computational results of the normal stress profiles are different from the existing measurements of the normal stress profiles within a flat plate turbulent boundary layer (Klebanoff, 1955).

The Reynolds shear stress profiles within the boundary layer at $\varphi = 0°$, 5°, and 10° were plotted in Figs. 8(a) and (b). These profiles show that the shear stress increases from the zero value at the boundary layer edge to a maximum value at $\eta \approx 1$ and then decreases to the boundary value at the surface. The shear stress also increases significantly within the boundary layer at the downstream locations.

The analytical results of the profiles of the dimensionless time-averaged correlation $-\overline{vt}/k_F^{0.5}T_F$ within the boundary layer at $\varphi = 0°$, 5°, and 10° are shown in Figs. 9(a) and (b). These profiles are similar to the shear stress profiles in Figs. 8(a) and (b). The turbulence correlation also increases as the flow moves downstream. With a large Tu in the free stream (Fig. 9(a)), small variations in the $-\overline{vt}$ profiles occur within the downstream boundary layer. However, the profiles in Fig. 9(b) show that, with a small Tu in the free stream, the $-\overline{vt}$ correlation increases within the boundary layer at the downstream locations. Since $k \propto Tu^2$, these profiles also indicate that a large Tu or a large Re in the free stream can induce a large level of the $-\overline{vt}$ correlation within the boundary layer.

Surface Heat Transfer and Skin Friction

The present analytical results of the Nusselt number and the skin friction factor within 10° of the stagnation point are shown in Figs. 10(a),and (b). These results are compared with the stagnation-point Nusselt number from the existing experiment (Lowery and Vachon, 1975) and the skin friction factor from the laminar boundary layer flow analysis (Schlichting, 1968). The present analytical results of the stagnation-point Nusselt number are in good agreement with the experiment, with $Tu \leq 0.055$. For the case of $Tu = 0.110$, the present analyses predict a lower level of the stagnation-point Nusselt number than the measurement. Since similar level of the Nusselt number was also measured by O'Brian and Vanfossen (1985), different length scale may be required in the analyses to calculate these experimental stagnation-point Nusselt numbers at $Tu = 0.110$. The present analytical results also show that the Nusselt number increases slightly at locations near the stagnation point and then remains constant at downstream locations. However, the skin friction factor increases continuously at the downstream locations. These surface phenomena are consistent with the variations of the boundary layer turbulence profiles (Figs. 4 and 5). Although the turbulence correlations $-\overline{uv}$ and $-\overline{vt}$ have decreased to zero at the boundary layer edge, Reynolds normal stresses occur within the boundary layer. These normal stresses interact with the mean velocity and the mean temperature to produce turbulence correlations $-\overline{uv}$ and $-\overline{vt}$ within the boundary layer. Therefore, depending on the free-stream velocity turbulence, the present analysis predicts larger surface heat transfer rate and skin friction than those with laminar flow conditions.

To show the effect of the free-stream turbulence longitudinal microlength scale on the surface heat transfer rate, some computational results for the cases with $Re = 2.52 \times 10^5$, $Tu = 0.028$, and different $\lambda_F/D = 0.0053$ and 0.0079 are compared in Figs. 11(a) to (d). With a small λ_F/D (= 0.0053) in the free-stream turbulence, small amplification in K_2 and attenuations in K_1 and K_3 were predicted along the stagnation-point streamline (Fig. 11(a)). With a large λ_F/D (= 0.0079), the Reynolds normal stresses amplified along the stagnation-point streamline in the external flow and these normal stresses induced large turbulence correlation $-\overline{vt}$ within the boundary layer and mean temperature gradient at the surface (Fig. 11(b)).

The variations of the turbulence kinetic energy along the stagnation-point streamline are also shown in Fig. 11(a). Depending on the free-stream turbulence microlength scale, the turbulence kinetic energy can increase or decrease as the flow moves toward the stagnation point. With a small λ_F/D, the free-stream turbulence has a large turbulence dissipation rate. This large dissipation rate is the dominant factor in the development of the turbulence and the turbulence kinetic energy is reduced. A smaller K_e, as it is compared with K_F, occurs along the boundary layer edge and this small turbulence kinetic energy induces a low level of the turbulence correlation $-\overline{vt}$ within the boundary layer. Therefore, small mean temperature gradient and heat transfer rate occur at the surface (Figs. 11(b) and (c)). For the case with a large free-stream turbulence microlength scale, the production term is the dominant factor in the turbulence development and the turbulence kinetic energy is increased. Therefore, a large turbulence kinetic energy occurs at the boundary layer edge and this turbulence kinetic energy induces a high level of the turbulence correlation $-\overline{vt}$ within the boundary layer. Therefore, large mean temperature gradient and heat transfer rate occur at the surface (Figs. 11(b) and (c)). With $\lambda_F/D = 0.0079$ in the free-stream turbulence, the present analysis predicted the stagnation-point Froessling number reported by Lowery and Vachon (1975).

Smith and Kuethe (1966) and Zukauskas and Ziugzda (1985) also performed the experiments of the stagnation-point surface heat transfer rates due to circular cylinders in turbulent freestream. These existing experimental results have been used by many researchers to verify their analyses of the stagnation-point flow. The present analysis was also used to predict these existing measurements of the stagnation-point heat transfer rates. Since details of the free-stream turbulence length scales were not reported in these studies, the present analysis could not be used to calculate the turbulence kinetic energy along the stagnation-point streamline within the external flow. However, overall heat transfer results could be attempted. The assumption that the boundary layer edge turbulence kinetic energy is proportional to the free-stream turbulence kinetic energy was made to perform the boundary layer flow analysis. The computational results, based on three different K_e/K_F ratios, of the stagnation-point heat transfer rates are compared with the various measurements in Fig. 11(d). These

results are presented in terms of the correlation parameters $TuRe^{0.5}$ and $NuRe^{-0.5}$. With $K_e/K_F = 1$, the present analytical results agree with the experiments and the surface heat transfer correlation reported by Smith and Kuethe (1966). A smaller K_e, as it is compared with K_F, was required in the present analysis to predict the existing measurements of Lowery and Vachon (1975) and Zukauskas and Ziugzda (1985), especially for the cases with large $TuRe^{0.5}$. With a high turbulence intensity in the freestream, the turbulence is most likely to be anisotropic and is dominated by the turbulence along the V_F direction. The free-stream turbulence has a lower turbulence kinetic energy than that of an isotropic turbulence and it has a large turbulence dissipation rate due to large v_F^2. With a large free-stream turbulence dissipation rate, the turbulence kinetic energy is reduced as the flow moves along the stagnation-point streamline. A small turbulence kinetic energy occurs at the boundary layer edge and this turbulence kinetic energy induces a low surface heat transfer rate. Therefore, $K_e < K_F$ is required in the present boundary layer flow analysis to predict the experiment with a large value of $TuRe^{0.5}$ in the freestream. It is also interesting to see that the present analysis can predict the experimental stagnation-point Froessling number (Zukauskas and Ziugzda, 1985) which is out of the range of the existing correlations by Smith and Kuethe (1966) and Lowery and Vachon (1975). This result is significant since the experiment by Zukauskas and Ziugzda (1985) was pressurized. The freestream Reynolds number was large and the boundary layer thickness over the cylinder surface was very thin in their tests.

The analysis of the length scale for the turbulence closure assumptions is another aspect of the turbulence modeling. In general, two different length scales are required. The length scales are related to each other through additional empirical constants and a turbulence Reynolds number (Donaldson et al., 1972). This type of analysis on the length scale was not pursued in this study. Based on the discussion of the length scales in the work by Donaldson et al. (1972), simple relations, Eq. (11), for a single length scale was used in the present analysis. However, the effect of the free-stream turbulence on the length scale was considered through the analysis of the boundary layer edge turbulence conditions. Equation (11) enabled the present analysis to predict satisfactorily the existing measurements of the stagnation-point heat transfer rates.

CONCLUSIONS

Boundary layer flow and turbulence transport analyses were formulated to study the development of the time-averaged double correlations of the velocity and temperature fluctuations and the mean flow properties in the stagnation-point flow of a circular cylinder in a turbulent freestream. Steady and incompressible turbulent boundary layer flow equations, the $k - \varepsilon$ two-equation turbulence modeling and the Reynolds stress transport equations were used to formulate the theoretical models. The boundary layer edge turbulence conditions and the length scale for the turbulence closure assumptions were also obtained analytically by matching the turbulence boundary conditions. With the assumption of an isotropic free-stream turbulence, the analyses were used to calculate numerically the surface heat transfer rate, the skin friction and the boundary layer profiles of the mean velocity and the mean temperature in the stagnation-point flow. The present analytical results were then compared with the existing experiments to validate the theoretical models in the analysis.

The results of this study indicate that:

1. The time-averaged double correlation of the velocity and temperature fluctuations decays rapidly along the stagnation-point streamline within the external flow region. The turbulence correlation of the velocity and temperature fluctuations is very small at the boundary layer edge. Therefore, the free-stream temperature fluctuation does not appear to penetrate into the boundary layer and has no effect on the surface heat transfer rate.

2. With turbulence in the free stream, the Reynolds normal stresses may increase or decrease as the flow moves toward the surface along the stagnation-point streamline. However, large Reynolds normal stresses usually occur at the boundary layer edge. These Reynolds normal stresses induce the shear stress $-\overline{uv}$ and the turbulence thermal flux $-\overline{vt}$ within the boundary layer. These turbulence fluxes change the boundary layer mean velocity and mean temperature profiles and, thus, the surface heat transfer rate and the skin friction. Including the effect of the free-stream turbulence, the present analysis predicts larger levels of the surface heat transfer rate and the skin friction than those with laminar free-stream conditions.

3. The free-stream turbulence dissipation rate can influence the stagnation-point heat transfer rate. When the free-stream turbulence dissipation rate is large, the turbulence kinetic energy is reduced as the flow moves toward the boundary layer edge. Due to the small turbulence kinetic energy at the boundary layer edge, a small surface heat transfer rate occurs beneath the stagnation-point flow. The free-stream turbulence dissipation rate is found to be a factor in the difference of the stagnation-point heat transfer rates reported in the existing studies.

4. With the prescribed isotropic free-stream turbulence conditions, the present analysis calculates the existing experimental measurements of the stagnation-point heat transfer rate when the free-stream Reynolds number is in the order of 10^5 and the free-stream turbulence intensity is $\leq$10 percent. The present analysis can be used to calculate the turbulence and mean flow properties when the free-stream turbulence is anisotropic. However, it requires the free-stream Reynolds normal stresses and the free-stream turbulence dissipation rate.

REFERENCES

Beckwith, I.E., and Bushnell, D.M., 1968, "Detailed Description and Results of a Method for Computing Mean and Fluctuating Quantities in Turbulent Boundary Layers," NASA TN D-4815.

Donaldson, C.D., Sullivan, R.D., and Rosenbaum, H., 1972, "A Theoretical Study of the Generation of Atmospheric-Clear Air Turbulence," AIAA Journal, Vol. 10, No. 2, pp. 162-170.

Hijikata, K., Yoshida, H., and Mori, Y., 1982, "Theoretical and Experimental Study of Turbulence Effects on Heat Transfer Around the Stagnation Point of a Cylinder," Heat Transfer 1982, Vol. 3, U. Grigull, et al, eds., Hemisphere Publishing Corp., Washington, D.C., pp. 165-170.

Hinze, J.O., 1975, Turbulence, 2nd edition, McGraw-Hill, New York.

Kestin, J., and Richardson, P.D., 1969, "The Effects of Free-Stream Turbulence and of Sound Upon Heat Transfer," ARL-69-0062, Wright-Patterson AFB, Dayton, OH. (Avail. NTIS, AD-691497).

Klebanoff, P.S., 1955, "Characteristics of Turbulence in a Boundary Layer with Zero Pressure Gradient," NACA Rept. 1247.

Launder, B.E., and Spalding, D.B., 1974, "The Numerical Computation of Turbulent Flows," Computer Methods in Applied Mechanics and Engineering, Vol. 3, No. 2, pp. 269-289.

Lowery, G.W., and Vachon, R.I., 1975, "The Effect of Turbulence on Heat Transfer from Heated Cylinders," International Journal of Heat and Mass Transfer, Vol. 18, No. 11, pp. 1229-1242.

O'Brien, J.E., and Vanfossen, G.J., 1985, "The Influence of Jet-Grid Turbulence on Heat Transfer From the Stagnation Region of a Cylinder in Crossflow," ASME Paper 85-HT-58. (NASA TM-87011).

Schlichting, H., 1968, Boundary Layer Theory, 6th ed., McGraw-Hill, New York, pp. 158-159.

Smith, M.C., and Kuethe, A.M., 1966, "Effects of Turbulence on Laminar Skin Friction and Heat Transfer," Physics of Fluids, Vol. 9, No. 12, pp. 2337-2344.

Strahle, W.C., 1985, "Stagnation Point Flows with Freestream Turbulence - The Matching Condition," AIAA Journal, Vol. 23, No. 11, pp. 1822-1824.

Traci, R.M., and Wilcox, D.C., 1975, "Freestream Turbulence Effects on Stagnation Point Heat Transfer," AIAA Journal, Vol. 13, No. 7, pp. 890-896.

Wang, C.R., and Yeh, F.C., 1987, "Application of Turbulence Modeling to Predict Surface Heat Transfer in Stagnation Flow Region of Circular Cylinder," NASA TP-2758. (ASME HTD-Vol. 87, pp. 35-48.)

Zukauskas, A., and Ziugzda, J., 1985, Heat Transfer of a Cylinder in Crossflow, Hemisphere Publishing Corp., Washington, D.C.

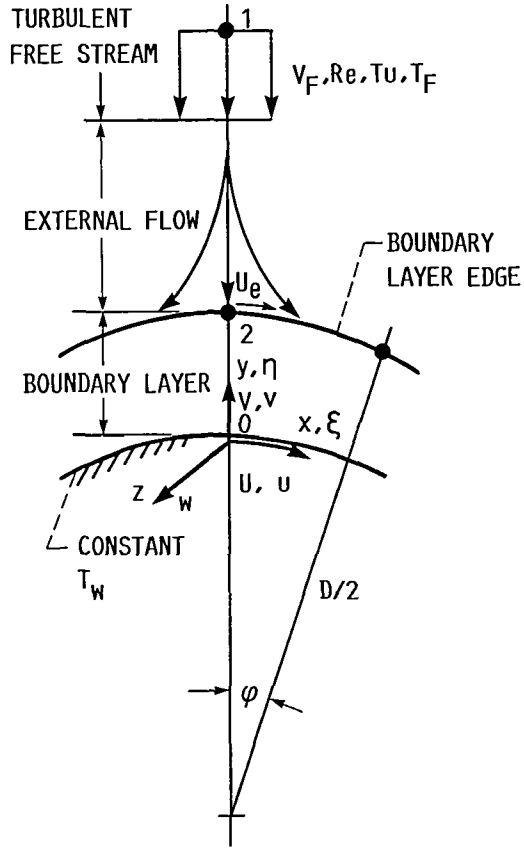

FIGURE 1. - SCHEMATIC OF FLOW FIELD OF INTEREST.

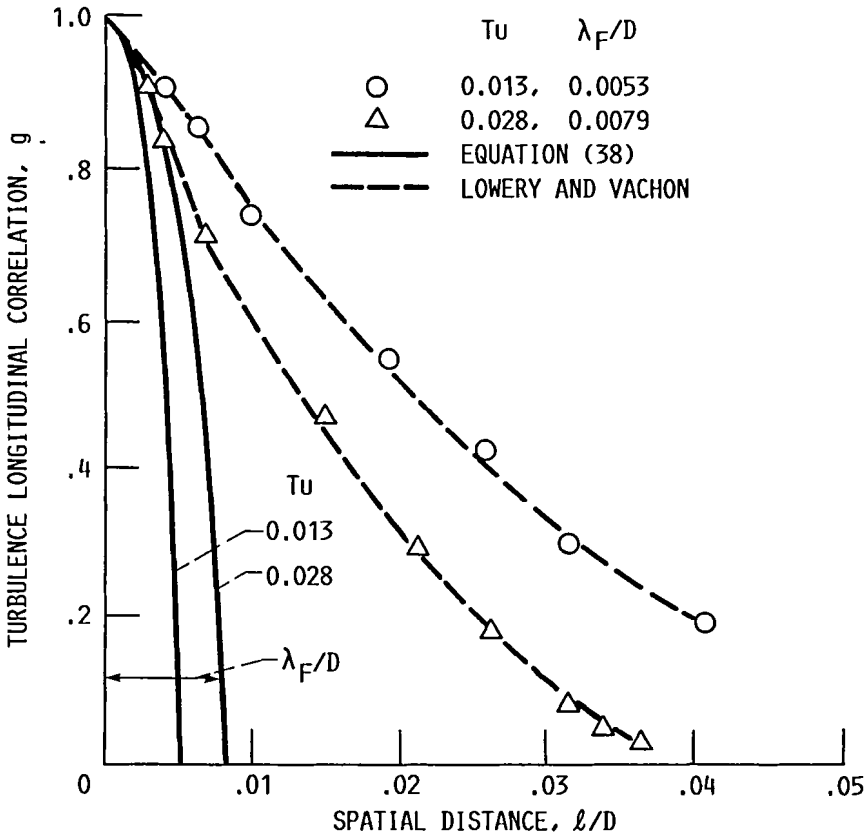

FIGURE 2. - FREE-STREAM TURBULENCE LONGITUDINAL MICRO-LENGTH SCALE, REYNOLDS NUMBER, Re = 2.52 x 10^5.

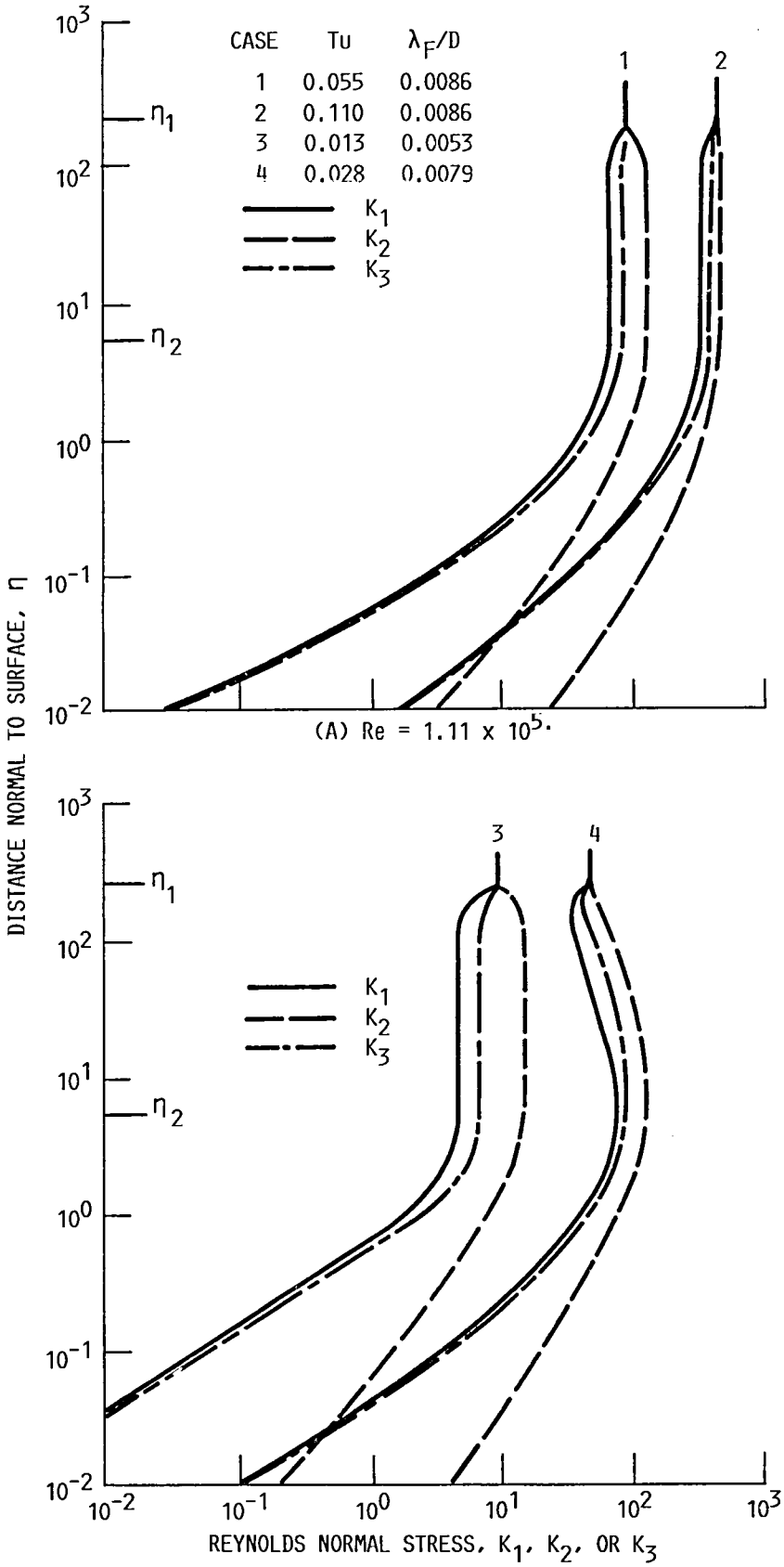

(A) Re = 1.11×10^5.

(B) Re = 2.52×10^5.

FIGURE 3. - VARIATIONS OF REYNOLDS NORMAL STRESSES ALONG STAGNATION-POINT STREAMLINE.

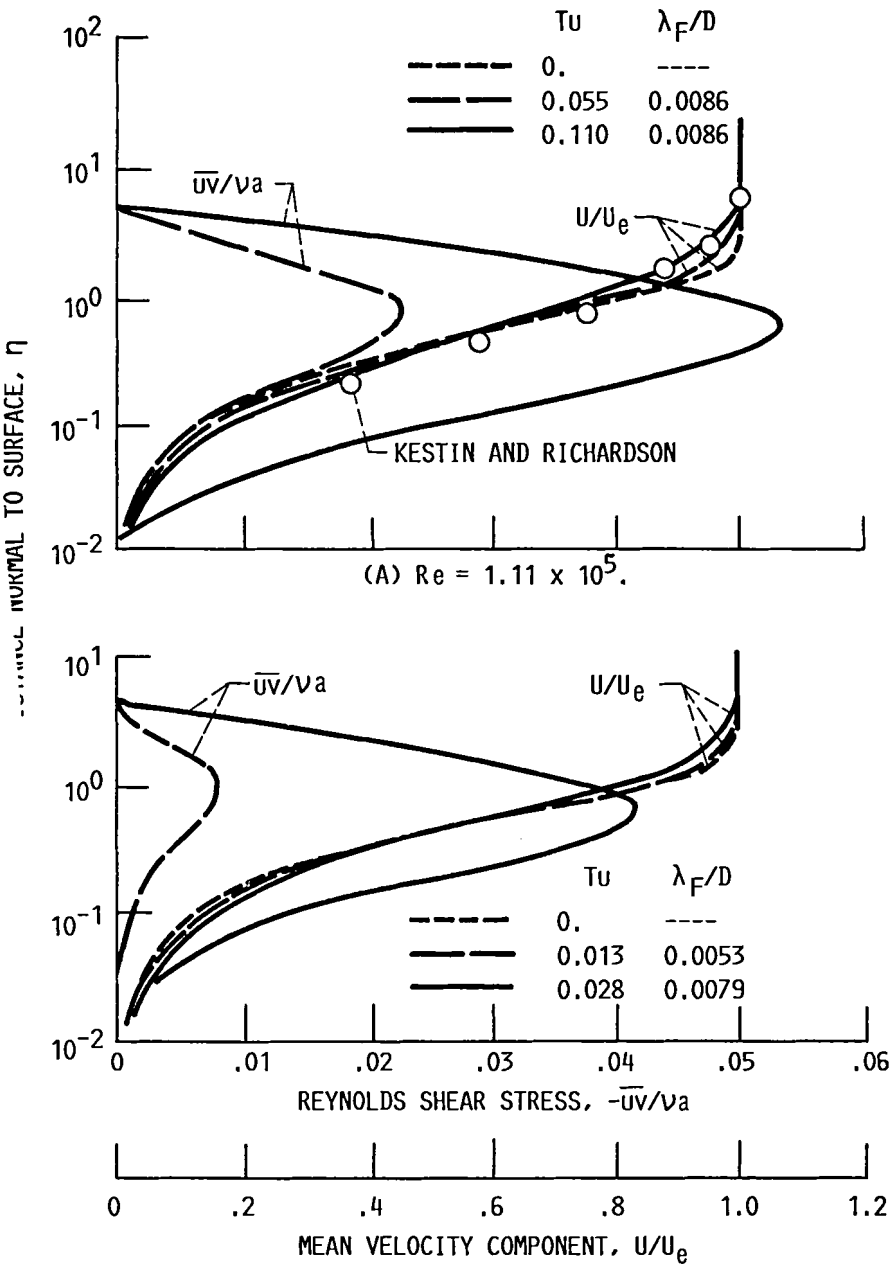

FIGURE 4. - VARIATIONS OF MEAN VELOCITY AND REYNOLDS SHEAR STRESS WITHIN BOUNDARY LAYER ALONG THE STAGNATION-POINT STREAMLINE.

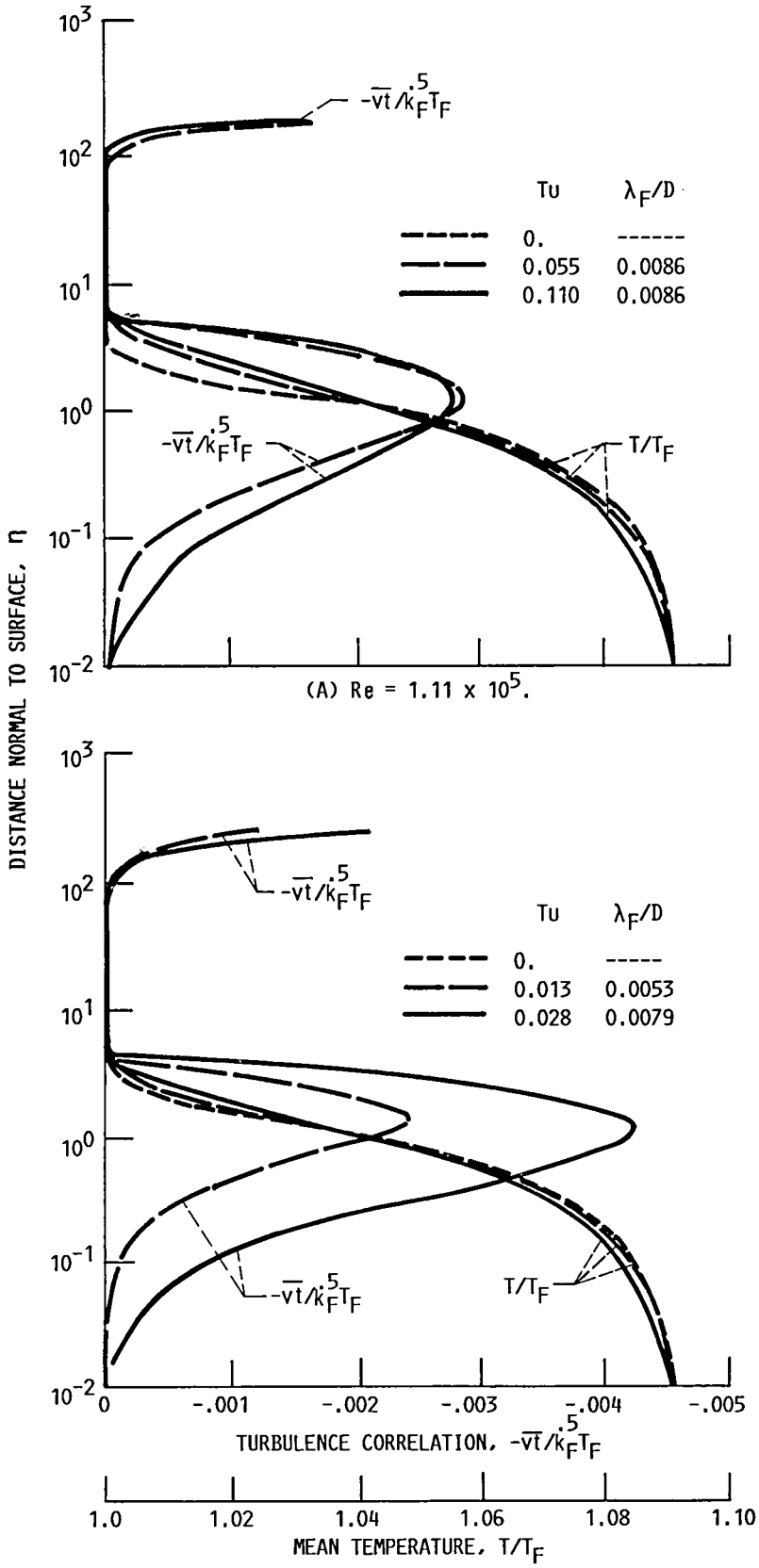

FIGURE 5. - VARIATIONS OF MEAN TEMPERATURE AND THE TURBULENCE CORRELATION WITHIN BOUNDARY LAYER ALONG STAGNATION-POINT STREAMLINE.

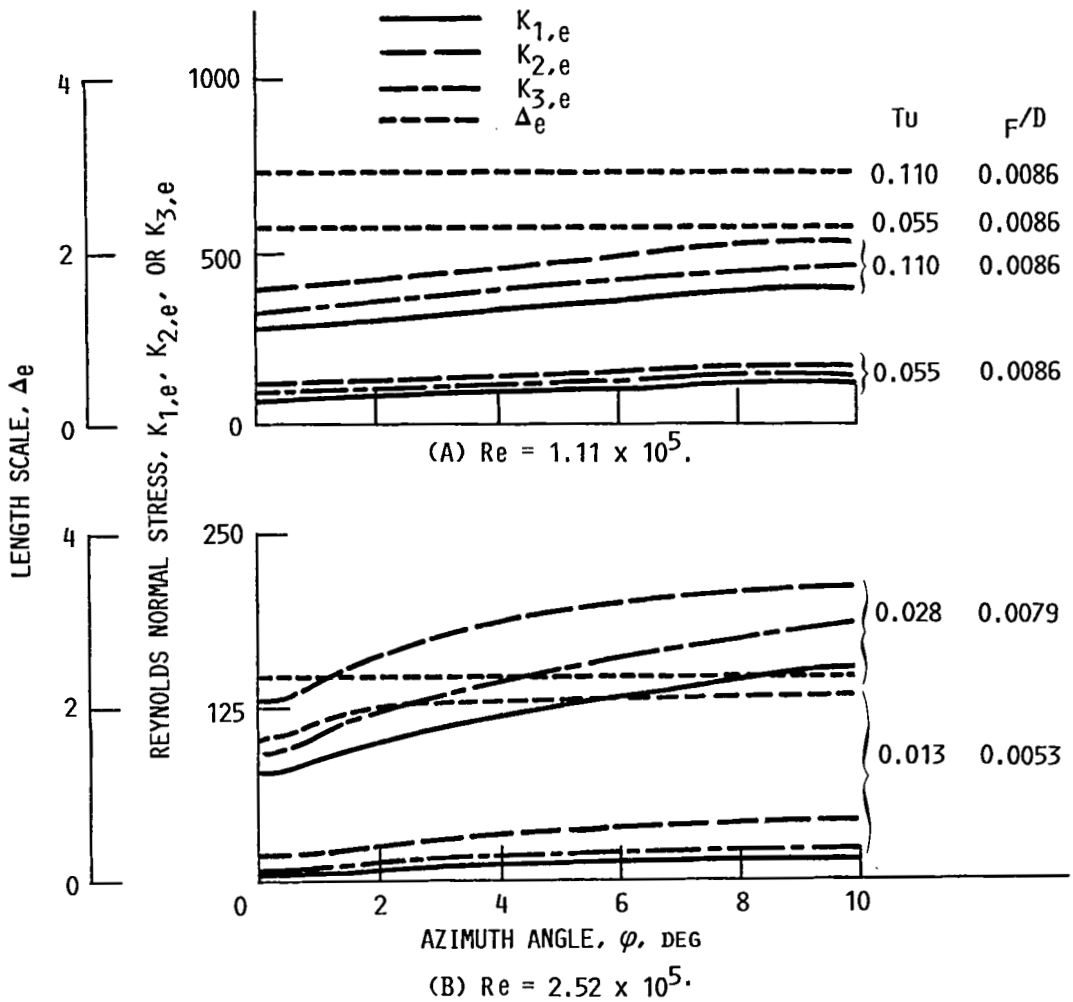

FIGURE 6. - VARIATIONS OF REYNOLDS NORMAL STRESSES AND LENGTH SCALE FOR TURBULENCE CLOSURE ASSUMPTION ALONG BOUNDARY LAYER EDGE.

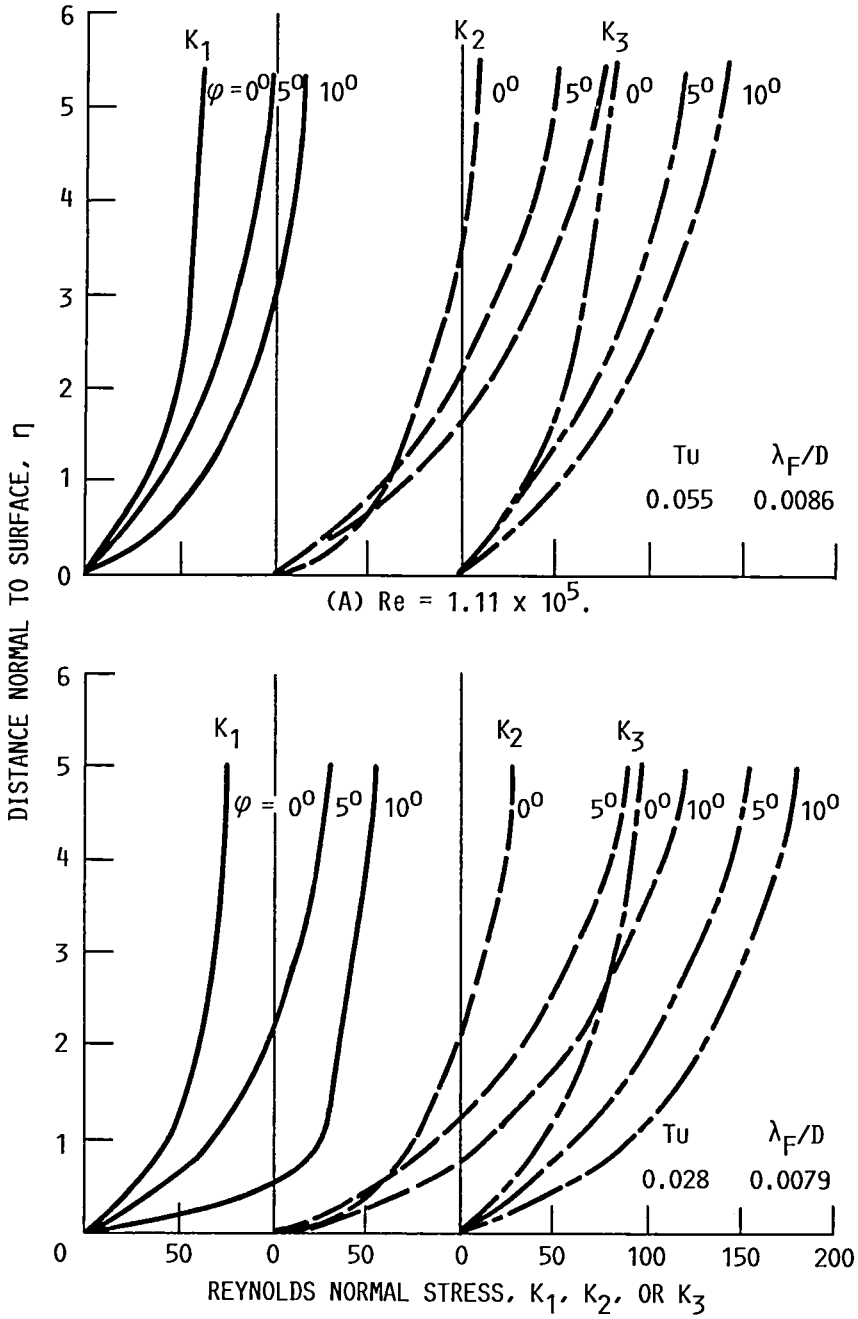

FIGURE 7. - REYNOLDS NORMAL STRESS PROFILES WITHIN BOUNDARY LAYER AT DOWNSTREAM LOCATIONS.

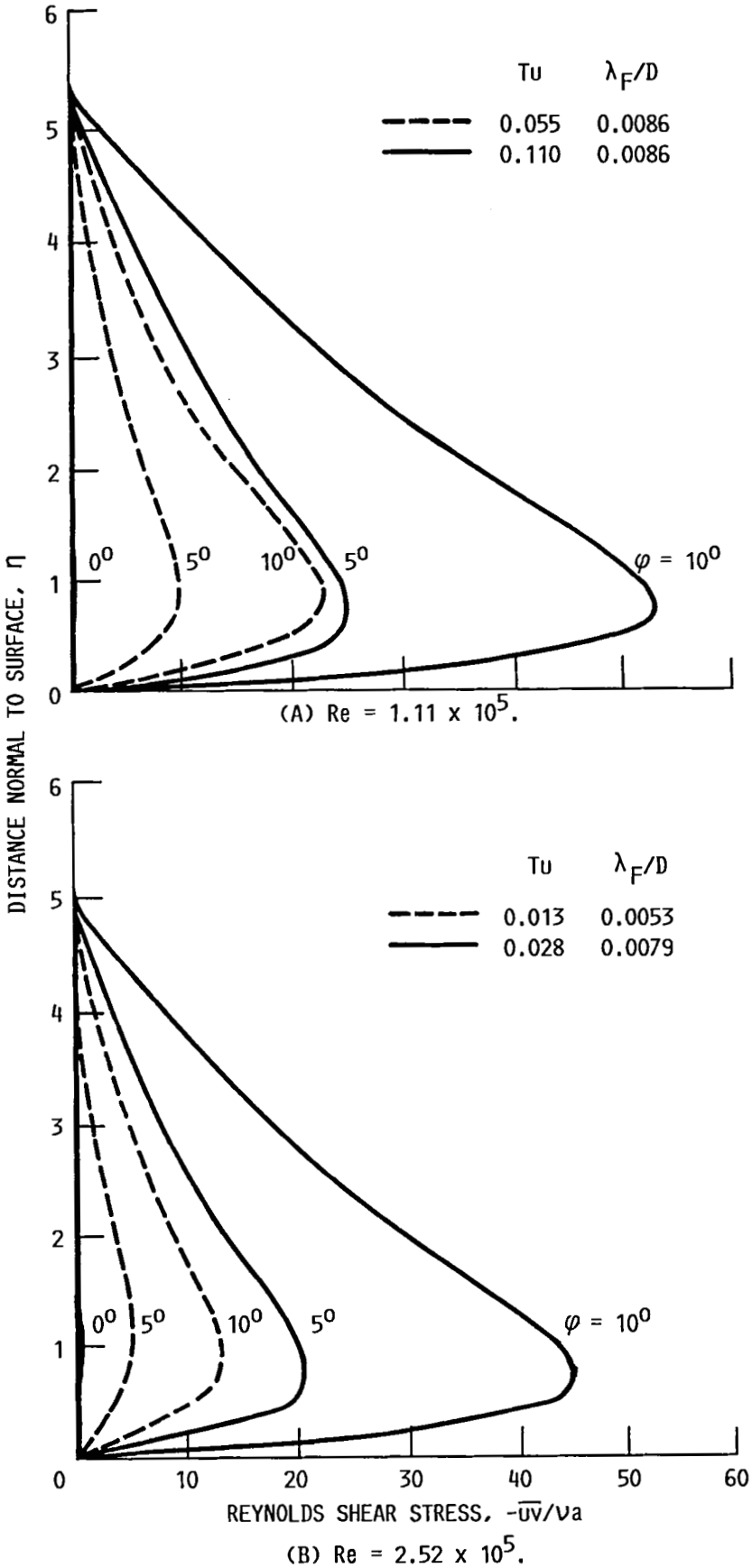

FIGURE 8. - REYNOLDS SHEAR STRESS PROFILES WITHIN BOUNDARY LAYER AT DOWNSTREAM LOCATIONS.

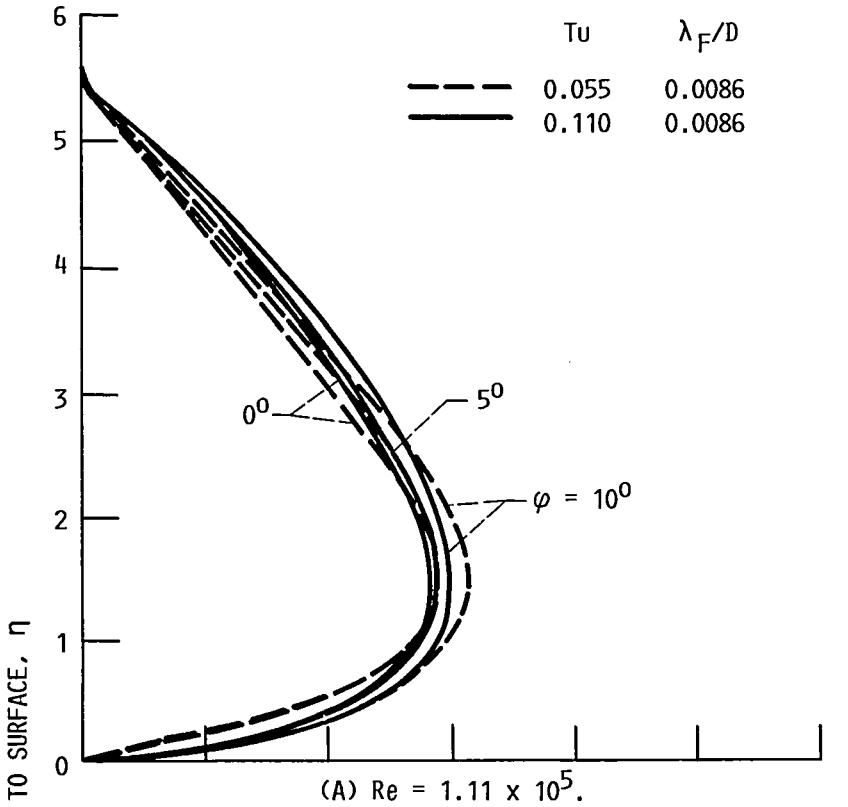

(A) Re = 1.11×10^5.

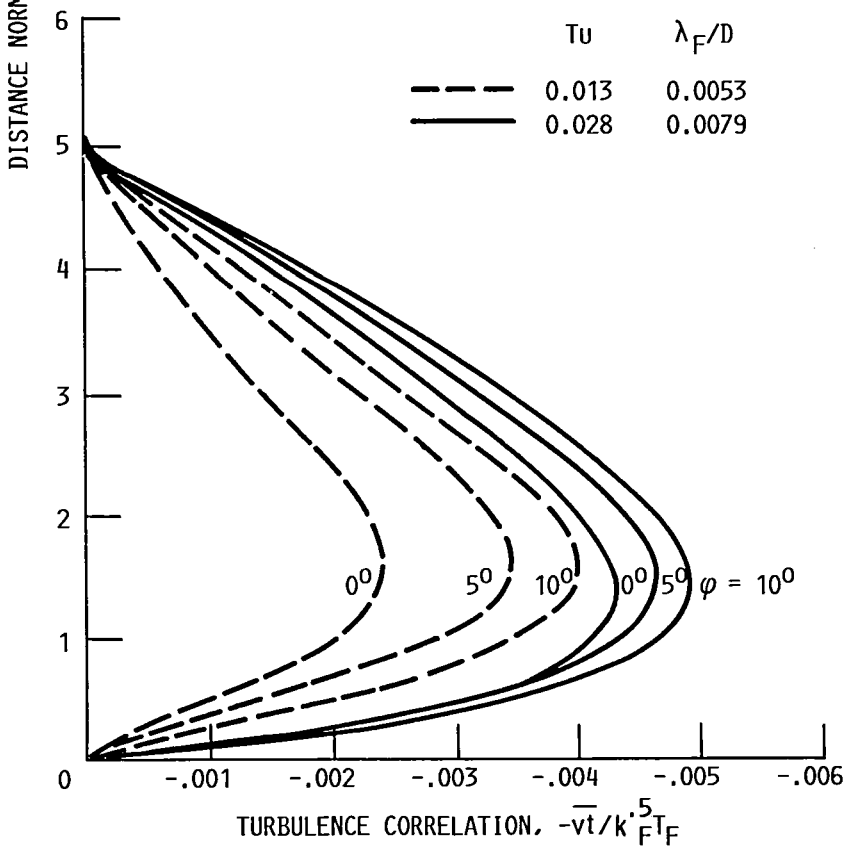

(B) Re = 2.52×10^5.

FIGURE 9. - PROFILES OF TURBULENCE CORRELATION - $\overline{vt}$ WITHIN BOUNDARY LAYER AT DOWNSTREAM LOCATIONS.

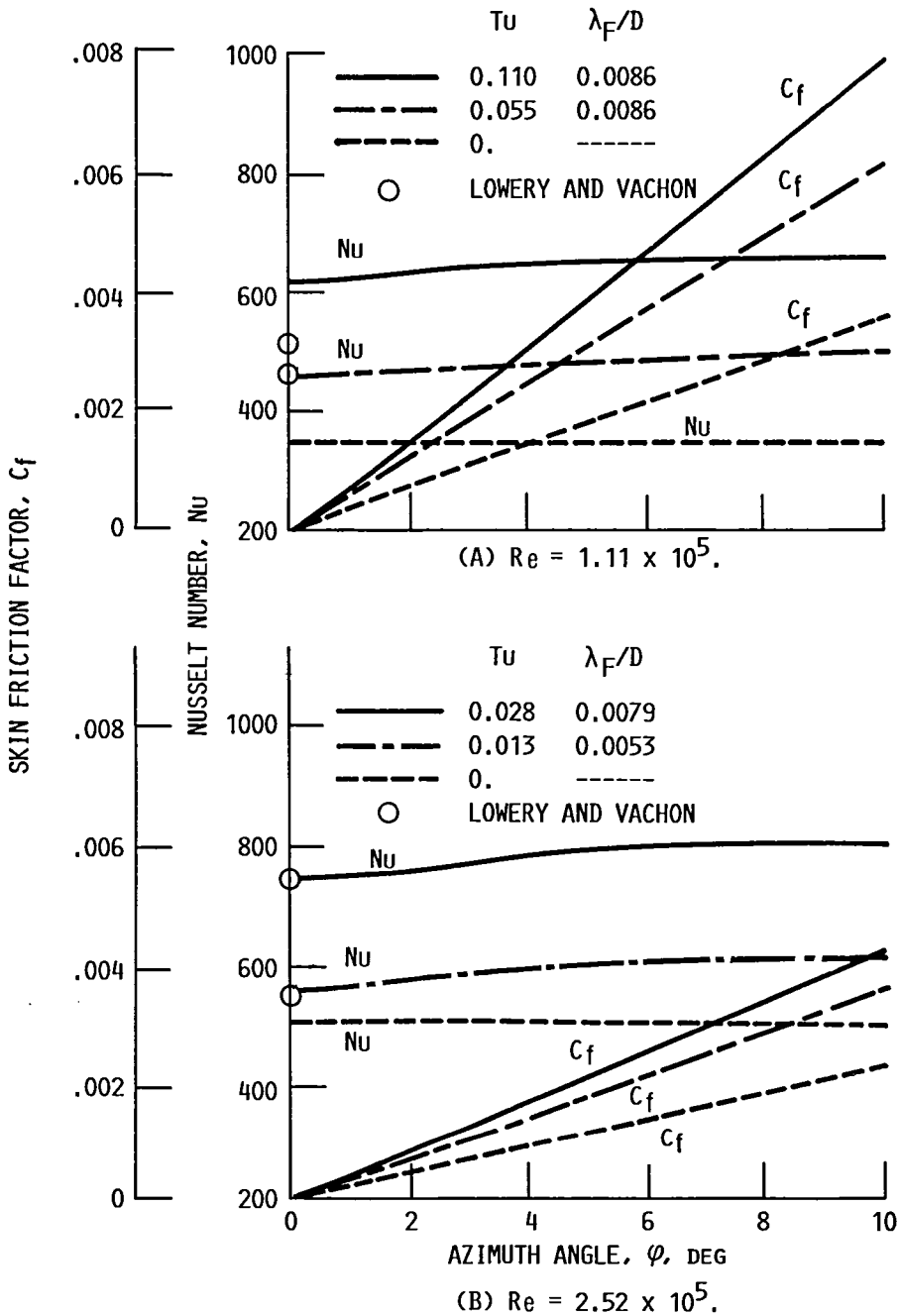

FIGURE 10. - NUSSELT NUMBER AND SKIN FRICTION FACTOR AT LOCATIONS NEAR STAGNATION-POINT.

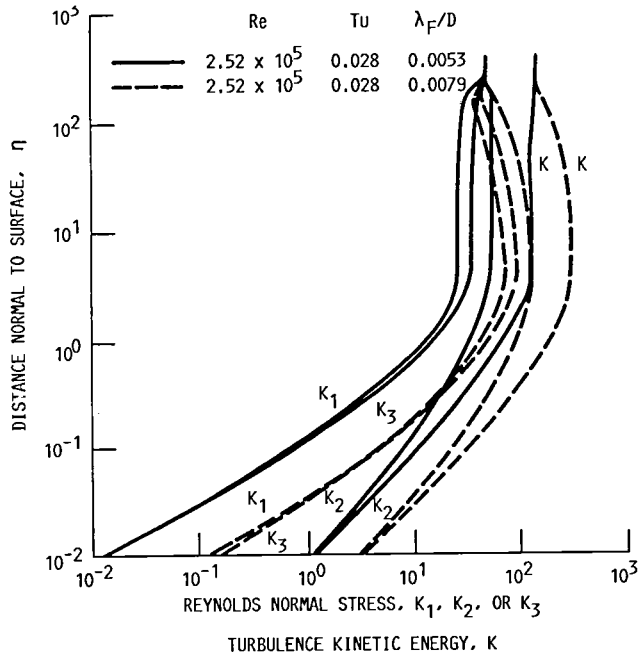

(A) REYNOLDS NORMAL STRESSES AND TURBULENCE KINETIC ENERGY.

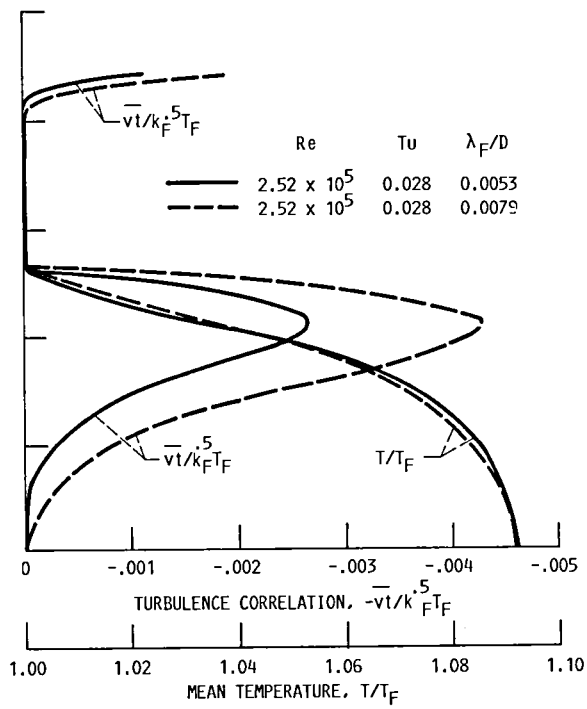

(B) MEAN TEMPERATURE AND TURBULENCE CORRELATION.

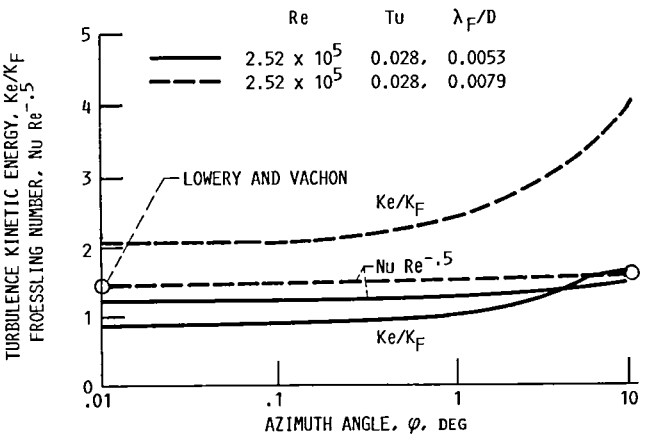

(C) BOUNDARY LAYER EDGE TURBULENCE KINETIC ENERGY AND FROESSLING NUMBER AT LOCATIONS NEAR STAGNATION POINT.

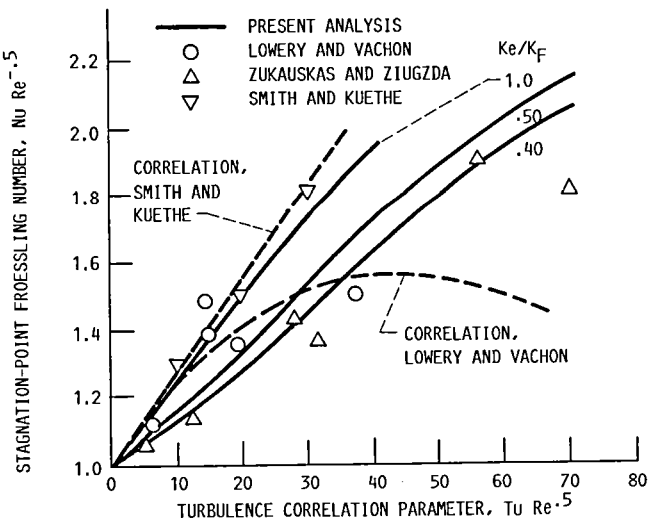

(D) STAGNATION-POINT HEAT TRANSFER CORRELATIONS.

FIGURE 11. - EFFECT OF FREE-STREAM TURBULENCE LENGTH SCALE ON TURBULENCE CORRELATIONS, MEAN TEMPERATURE PROFILES, AND STAGNATION-POINT HEAT TRANSFER CORRELATIONS.

NASA
National Aeronautics and Space Administration

Report Documentation Page

1. Report No.	2. Government Accession No.	3. Recipient's Catalog No.
NASA TM-100930		

4. Title and Subtitle

Correlations of Velocity and Temperature Fluctuations in the Stagnation-Point Flow of Circular Cylinder in Turbulent Flow

5. Report Date

6. Performing Organization Code

7. Author(s)

Chi R. Wang

8. Performing Organization Report No.

E-4201

10. Work Unit No.

505-62-21

9. Performing Organization Name and Address

National Aeronautics and Space Administration
Lewis Research Center
Cleveland, Ohio 44135-3191

11. Contract or Grant No.

13. Type of Report and Period Covered

Technical Memorandum

12. Sponsoring Agency Name and Address

National Aeronautics and Space Administration
Washington, D.C. 20546-0001

14. Sponsoring Agency Code

15. Supplementary Notes

Prepared for the 1988 Winter Annual Meeting of the American Society of Mechanical Engineers, Chicago, Illinois, November 28 - December 2, 1988.

16. Abstract

Boundary layer flow and turbulence transport analyses to study the influence of the free-stream turbulence on the surface heat transfer rate and the skin friction around the stagnation point of a circular cylinder in a turbulent flow are presented. The analyses are formulated with the turbulent boundary layer equations, the Reynolds stress transport equations and the $k - \varepsilon$ two-equation turbulence modeling. The analyses are used to calculate the time-averaged turbulence double correlations, the mean flow properties, the surface heat transfer rate and the skin friction with an isotropic turbulence in the freestream. The analytical results are described and compared with the existing experimental measurements. Depending on the free-stream turbulence properties, the turbulence kinetic energy can increase or decrease as the flow moves toward the surface. However, the turbulence kinetic energy induces large Reynolds normal stresses at the boundary layer edge. The Reynolds normal stresses change the boundary layer profiles of the time-averaged double correlations of the velocity and temperature fluctuations, the surface heat transfer rate and the skin friction. The free-stream turbulence dissipation rate can affect the stagnation-point heat transfer rate but the influence of the free-stream temperature fluctuation on the heat transfer rate is insignificant.

17. Key Words (Suggested by Author(s))	18. Distribution Statement
Heat transfer Boundary layer Turbulence	Unclassified - Unlimited Subject Category 02

19. Security Classif. (of this report)	20. Security Classif. (of this page)	21. No of pages	22. Price*
Unclassified	Unclassified	22	A02

NASA FORM 1626 OCT 86

*For sale by the National Technical Information Service, Springfield, Virginia 22161